

# Double-Sided Information Aided Temporal-Correlated Massive Access

Weifeng Zhu, *Graduate Student Member, IEEE*, Meixia Tao, *Fellow, IEEE*, and Yunfeng Guan

**Abstract**—This letter considers temporal-correlated massive access, where each device, once activated, is likely to transmit continuously over several consecutive frames. Motivated by that the device activity at each frame is correlated to not only its previous frame but also its next frame, we propose a double-sided information (DSI) aided joint activity detection and channel estimation algorithm based on the approximate message passing (AMP) framework. The DSI is extracted from the estimation results in a sliding window that contains the target detection frame and its previous and next frames. The proposed algorithm demonstrates superior performance over the state-of-the-art methods.

**Index Terms**—Massive access, temporal correlation, approximate message passing (AMP), side information.

## I. INTRODUCTION

Massive machine-type communication (mMTC) is one of the main use cases of the 5G and beyond mobile communication systems for supporting Internet of Things (IoT) applications. It is featured by the massive number of IoT devices and their sporadic activities [1]. To enable massive connectivity, grant-free random access is introduced in 5G as a new random access technique where devices can access channel resources without undergoing a handshake process. Thereby, the signaling overhead can be efficiently reduced. However, the main technical challenge of grant-free random access is device activity detection and channel estimation.

By exploiting the sporadic nature of data traffic in mMTC, compressed sensing (CS) techniques have been widely utilized to perform activity detection and channel estimation jointly in the literature [1]. Among all these CS-based methods, the approximate message passing (AMP) based algorithms have demonstrated favorable performance at efficient computation complexity in [2]–[5]. The covariance-based method [6] is another popular approach for activity detection, which can outperform the conventional CS-based methods when the number of antennas is large.

In practical IoT environment, if a device is activated by a burst event, the device often transmits continuously for a certain time interval. In other words, once activated, it often remains active in the upcoming consecutive transmission frames. This suggests that the device activity is correlated in the time domain. By accounting such temporal correlation, the performance of activity detection and channel estimation can be improved by formulating the problem from the dynamic CS (DCS) perspective [7]–[9]. Specifically, the work [7] proposes a sequential AMP (S-AMP) algorithm for device activity detection by using the historical knowledge. In [8], a hybrid generalized AMP (HyGAMP) algorithm is employed to

account the device activity information from both the previous frame and the next frame to improve performance. Note that both [7] and [8] focus on the scenario where the base station (BS) has single antenna. In [9], a side information aided multiple measurement vector based AMP (SI-aided MMV-AMP) algorithm is proposed for both single-antenna and multiple-antenna scenarios. Here, the SI is defined as the estimation result in the previous frame. However, the algorithm only considers the SI from the single previous frame and thus the temporal correlation is not fully exploited.

This work aims to fully exploit the temporal correlation of device activity for further enhancing the joint activity detection and channel estimation performance. This is motivated by the fact that the activity of each device in a current frame is not only related to the activity in the previous frame (single side) but also correlated with the activity in the next frame (double sides). More specifically, if we know one device is active in the previous frame, then with a large probability it will be considered to be active in the current frame; but if we know that the device is active in both the previous and next frames, almost surely it is active in the current frame. Therefore, by exploiting the estimation results from the adjacent frames in double sides, one can further lift the performance of activity detection and channel estimation at each current frame.

To this end, we first introduce a sliding-window detection strategy to account the double-sided information (DSI) from the previous frame as well as the next frame. Then we propose a DSI-aided activity detection and channel estimation algorithm based on the AMP-SI framework proposed in [10]. The proposed activity detector employs the log likelihood ratio (LLR) test. Numerical results show that the proposed algorithm significantly outperforms the state-of-the-art algorithms by further exploiting the temporal correlation of device activity.

## II. SYSTEM MODEL

Consider a grant-free massive access system, where a very large number  $N$  of single-antenna user devices communicate with a common  $M$ -antenna BS through a shared uplink channel. Due to the sporadic communication traffic, only a small subset of devices are activated in each transmission frame. Each frame consists of two phases, a pilot phase and a data phase. We concentrate on the pilot phase for activity detection and channel estimation. A unique pilot sequence  $\mathbf{a}_n = [a_{n,1}, a_{n,2}, \dots, a_{n,L}]^T \in \mathbb{C}^{L \times 1}$  is pre-allocated to each device  $n$ ,  $\forall n \in \{1, \dots, N\}$ , for identification and channel estimation, where  $L \ll N$  is the pilot length. We assume that the elements of each pilot sequence are generated following the independent and identically distributed (i.i.d.) complex Gaussian distribution with zero mean and variance  $\frac{1}{L}$ , i.e.,  $a_{n,l} \sim \mathcal{CN}(0, \frac{1}{L}), \forall n, l$ .

The authors are with the Department of Electronic Engineering, Shanghai Jiao Tong University, Shanghai 200240, China (e-mail: {wf.zhu, mxtao, yfguan69}@sjtu.edu.cn).

### A. Temporal-Correlated Activity Model

We consider temporally correlated device activity. Let  $\lambda_n^t \in \{0, 1\}$  denote the activity state of device  $n$  at the  $t$ th frame, with  $\lambda_n^t = 1$  meaning active and  $\lambda_n^t = 0$  otherwise. Without loss of generality, we assume  $\lambda_n^t$  evolves over  $t$  according to a stationary stochastic process and is i.i.d. for all devices. As in [7]–[9], the device activity evolution is modeled by a first-order steady Markov chain, which can be fully described by two transition probabilities  $p_{01} = \Pr(\lambda_n^{t+1} = 1 | \lambda_n^t = 0)$  and  $p_{11} = \Pr(\lambda_n^{t+1} = 1 | \lambda_n^t = 1)$ . Then the active probability of each device, denoted as  $p_a$ , in each frame can be derived by solving the eigenvalue problem as  $p_a = \frac{p_{01}}{1 - p_{11} + p_{01}}$ . Note that  $p_{01}$  and  $p_{11}$  can be estimated empirically based on the historical data. In the special case where  $p_{01} = p_{11}$ , the device activity is independent over time.

### B. Signal Model

We assume block-fading channel model where the channel of each device remains unchanged in one frame, but varies in different frames. In the  $t$ th frame, the channel coefficient vector between the BS and device  $n$  is defined as  $\mathbf{h}_n^t = \sqrt{\beta_n} \mathbf{g}_n^t \in \mathbb{C}^{1 \times M}$ , where  $\beta_n = \rho_n \gamma_n \in \mathbb{R}$  represents the large-scale fading coefficient affected by the attenuation factor  $\gamma_n$  and the transmit power  $\rho_n$ ,  $\mathbf{g}_n^t \in \mathbb{C}^{1 \times M}$  is the small-scale fading vector. This work adopts the simple power control strategy in [4] based on the attenuation factors to benefit cell-edge devices. Thus, we have  $\beta_n = \beta, \forall n$ . The small-scale fading is assumed to follow i.i.d. Rayleigh distribution, i.e.,  $\mathbf{g}_n^t \sim \mathcal{CN}(0, \mathbf{I}), \forall n, t$ . Then during the pilot phase, the received signals at the BS in the  $t$ th frame, denoted as  $\mathbf{Y}^t \in \mathbb{C}^{L \times M}$ , can be written as

$$\mathbf{Y}^t = \mathbf{A} \mathbf{\Lambda}^t \mathbf{H}^t + \mathbf{W}^t = \mathbf{A} \mathbf{X}^t + \mathbf{W}^t, \quad (1)$$

where  $\mathbf{A} = [\mathbf{a}_1, \mathbf{a}_2, \dots, \mathbf{a}_N] \in \mathbb{C}^{L \times N}$  is the pilot matrix;  $\mathbf{\Lambda}^t = \text{diag}([\lambda_1^t, \lambda_2^t, \dots, \lambda_N^t]^T) \in \mathbb{C}^{N \times N}$  is the activity matrix;  $\mathbf{H}^t = [(\mathbf{h}_1^t)^T, (\mathbf{h}_2^t)^T, \dots, (\mathbf{h}_N^t)^T]^T \in \mathbb{C}^{N \times M}$  is the channel matrix;  $\mathbf{X}^t = \mathbf{\Lambda}^t \mathbf{H}^t \in \mathbb{C}^{N \times M}$  represents the effective channel matrix;  $\mathbf{W}^t \in \mathbb{C}^{L \times M}$  is the additive noise matrix whose elements satisfy i.i.d. complex Gaussian distribution with zero mean and variance  $\sigma_w^2$ .

To perform activity detection and channel estimation is essential to recover  $\mathbf{X}^t$  from  $\mathbf{Y}^t$ . The problem can usually solved by the AMP algorithm with vector shrinkage function (vAMP) [2], [3]. This approach, however, treat  $\mathbf{X}^t$  in different frames independently and thus ignores the temporal correlation. In the following, we propose to leverage the temporal correlation of device activity by exploiting the double-sided information under the vAMP framework.

## III. VAMP FRAMEWORK WITH SIDE INFORMATION

### A. Overview of the SI-Aided vAMP

In this subsection, we first introduce the SI-aided vAMP framework, denoted as vAMP-SI. The general procedure of the framework roots from the AMP algorithm with SI proposed in [10] and operates as follows. Let  $\hat{\mathbf{X}}_i^t$  denote the estimation of the effective channel  $\mathbf{X}^t$  in the  $i$ th iteration. Also, let  $\mathbf{V}_i^t$  denote the residual of the received signal  $\mathbf{Y}^t$  corresponding to

the estimation  $\hat{\mathbf{X}}_i^t$ . Starting with  $\hat{\mathbf{X}}_0^t = \mathbf{0}$  and  $\mathbf{V}_0^t = \mathbf{Y}^t$ , the algorithm computes at the  $i$ th iteration:

$$\mathbf{R}_i^t = \hat{\mathbf{X}}_{i-1}^t + \mathbf{A}^H \mathbf{V}_{i-1}^t, \quad (2)$$

$$\hat{\mathbf{X}}_i^t = \boldsymbol{\eta}_i(\mathbf{R}_i^t, \mathcal{S}^t), \quad (3)$$

$$\mathbf{V}_i^t = \mathbf{Y}^t - \mathbf{A} \hat{\mathbf{X}}_i^t + \frac{1}{L} \mathbf{V}_{i-1}^t \sum_{n=1}^N \frac{\partial \boldsymbol{\eta}_{n,i}(\mathbf{r}_{n,i}^t, \mathcal{S}_n^t)}{\partial \mathbf{r}_{n,i}^t}, \quad (4)$$

where  $\mathbf{R}_i^t \in \mathbb{C}^{N \times M}$  can be viewed as the matched filtered output on the iteration- $(i-1)$  residual measurement  $\mathbf{V}_{i-1}^t$ ;  $\mathcal{S}^t = \{\mathcal{S}_n^t\}_{n=1}^N$  with each  $\mathcal{S}_n^t$  being the SI to improve the recovery quality of  $\mathbf{x}_n^t$  for each device  $n$ ;  $\boldsymbol{\eta}_i(\cdot, \mathcal{S}^t) = [(\boldsymbol{\eta}_{1,i}(\cdot, \mathcal{S}_1^t))^T, \dots, (\boldsymbol{\eta}_{N,i}(\cdot, \mathcal{S}_N^t))^T]^T$  with each  $\boldsymbol{\eta}_{n,i}(\cdot, \mathcal{S}_n^t) : \mathbb{C}^{1 \times M} \rightarrow \mathbb{C}^{1 \times M}$  being the SI-aware shrinkage function that operates on the  $n$ th row of  $\mathbf{R}_i^t$ , denoted as  $\mathbf{r}_{n,i}^t$ . Note that the residual calculation in (4) also includes the ‘‘Onsager correction’’ term  $\frac{1}{L} \mathbf{V}_{i-1}^t \sum_{n=1}^N \frac{\partial \boldsymbol{\eta}_{n,i}(\mathbf{r}_{n,i}^t, \mathcal{S}_n^t)}{\partial \mathbf{r}_{n,i}^t}$ .

The key difference between vAMP-SI and vAMP lies in the introduction of SI in the shrinkage function  $\boldsymbol{\eta}_{n,i}(\cdot, \mathcal{S}_n^t)$ . Thus, the definition of SI plays a vital role in the vAMP-SI framework. According to the activity model in Section II-A, the activity of each device  $n$  in the current frame is correlated to those in the previous and next frames. This motivates us to extract the SI from the estimation results in these two frames.

### B. SI Acquisition

Similar to [9], the considered SI in this paper is identified from the state evolution of vAMP-SI in the asymptotic regime where  $L, N \rightarrow \infty$  with fixed  $L/N$  and  $p_a$ . In specific, at the estimation of  $\mathbf{x}_n^t$  for each device  $n$  in each  $i$ th iteration, the matched filtered output  $\mathbf{r}_{n,i}^t$  in the AMP-based algorithm can be accurately modeled by

$$\mathbf{r}_{n,i}^t = \mathbf{x}_n^t + \mathbf{d}_{n,i}^t (\boldsymbol{\Sigma}_{i-1}^t)^{\frac{1}{2}}, \quad (5)$$

where  $\mathbf{x}_n^t \in \mathbb{C}^{1 \times M}$  is the  $n$ th row of  $\mathbf{X}^t$ ,  $\mathbf{d}_{n,i}^t \in \mathbb{C}^{1 \times M}$  is the corrupting noise whose elements follow i.i.d.  $\mathcal{CN}(0, 1)$ ,  $\boldsymbol{\Sigma}_i^t \in \mathbb{C}^{M \times M}$  is the covariance matrix of  $\mathbf{r}_{n,i}^t$ . Here,  $\boldsymbol{\Sigma}_i^t$  is also known as the *state* of vAMP-SI in the  $i$ th iteration and it evolves as

$$\boldsymbol{\Sigma}_i^t = \sigma_w^2 \mathbf{I} + \frac{N}{L} \mathbb{E} [(\mathbf{q}_{n,i-1}^t)^H \mathbf{q}_{n,i-1}^t], \quad (6)$$

where  $\mathbf{q}_{n,i-1}^t = \boldsymbol{\eta}_{n,i-1}(\mathbf{x}_n^t + \mathbf{d}_{n,i}^t (\boldsymbol{\Sigma}_{i-1}^t)^{\frac{1}{2}}, \mathcal{S}_n^t) - \mathbf{x}_n^t$ . Here, the expectation is performed over both  $\mathbf{x}_n^t$  and  $\mathbf{d}_{n,i}^t$ .

Let  $\mathbf{R}_{n,\infty}^t = [\mathbf{r}_{1,\infty}^t]^T, \dots, (\mathbf{r}_{N,\infty}^t)^T]^T$  and  $\boldsymbol{\Sigma}_{n,\infty}^t$  denote the converged matched filtered output and the converged state in vAMP-SI in each frame  $t$ . According to (5), the statistical relationship between  $\mathbf{r}_{n,\infty}^t$  and  $\mathbf{x}_n^t$  can be modeled as

$$\mathbf{r}_{n,\infty}^t = \mathbf{x}_n^t + \mathbf{d}_{n,\infty}^t (\boldsymbol{\Sigma}_{n,\infty}^t)^{\frac{1}{2}}, \quad (7)$$

where  $\mathbf{d}_{n,\infty}^t$  is the corrupting noise in the converged matched filtered output. At the same time, the Markov chain based activity model reveals the correlation between  $\mathbf{x}_n^t$  and  $(\mathbf{x}_n^{t-1}, \mathbf{x}_n^{t+1})$ , thus we can establish the correlation between  $\mathbf{x}_n^t$  and  $(\mathbf{r}_{n,\infty}^{t-1}, \mathbf{r}_{n,\infty}^{t+1})$ . Note that the SI in [9] is only extracted from  $\mathbf{x}_n^t$  and  $\mathbf{r}_{n,\infty}^{t-1}$ . In this work, we extract SI from the correlation

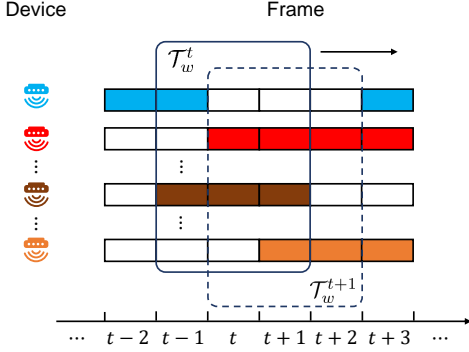


Fig. 1. The diagram of the sliding-window detection strategy

among  $\mathbf{x}_n^t$ ,  $\mathbf{r}_{n,\infty}^{t-1}$  and  $\mathbf{r}_{n,\infty}^{t+1}$ . Specifically, the estimation results of  $\mathbf{r}_{n,\infty}^{t-1}$  and  $\mathbf{r}_{n,\infty}^{t+1}$  are used as the SI for device  $n$ , denoted as  $\mathcal{S}_n^t = \{\mathbf{r}_{n,\infty}^{t-1}, \mathbf{r}_{n,\infty}^{t+1}\}$ , in the vAMP-SI framework<sup>1</sup>. In the following, we elaborate how to utilize the extracted SI for joint activity detection and channel estimation.

#### IV. DOUBLE-SIDED INFORMATION AIDED JOINT ACTIVITY DETECTION AND CHANNEL ESTIMATION

##### A. Sliding-Window Detection

As shown in Fig. 1, we perform joint activity detection and channel estimation in a sliding-window manner. The sliding window is defined as  $\mathcal{T}_w^t = \{t-1, t, t+1\}$ . It includes the target detection frame and the frames from which the SI is acquired. After finishing the detection and estimation in frame  $t$ , the window slides to  $\mathcal{T}_w^{t+1}$  to perform the task in the next frame. In each sliding window, there are totally  $2^3$  possible activity patterns for each device. We denote each pattern as  $\mathbf{P}_s = \lambda_n^{t-1} \lambda_n^t \lambda_n^{t+1}$ , and its occurrence probability as  $u_s = p(\mathbf{P}_s)$  for  $s = 1, \dots, 8$ . The occurrence probabilities can be obtained by using the first-order Markov chain based temporal correlation as modeled in Section II-A. For instance, we have  $u_s = (1-p_a)(1-p_{01})^2$  when  $\mathbf{P}_s = 000$  and  $u_s = pa p_{11}^2$  when  $\mathbf{P}_s = 111$ .

##### B. Shrinkage Function Design

Assuming that the system statistics are available, we can design the shrinkage function based on the minimum mean-squared error (MMSE) criterion, known as the MMSE-optimal denoising function, to achieve the Bayesian optimality. We first model the effective channel vectors  $\mathbf{x}_n^t$  of each user  $n$  in the sliding window  $\mathcal{T}_w^t$  with a multivariable Bernoulli Gaussian distribution. The probability distribution can be expressed as

$$p(\{\mathbf{x}_n^\tau\}_{\tau \in \mathcal{T}_w}) = \sum_{s=1}^8 \left[ u_s \cdot \left( \prod_{\tau=t-1}^{t+1} d_s(\mathbf{x}_n^\tau) \right) \right], \quad (8)$$

where

$$d_s(\mathbf{x}_n^\tau) = \begin{cases} \delta(\mathbf{x}_n^\tau), & \text{if } \lambda_n^\tau = 0 \text{ in } \mathbf{P}_s, \\ \mathcal{CN}(\mathbf{x}_n^\tau; 0, \beta), & \text{if } \lambda_n^\tau = 1 \text{ in } \mathbf{P}_s, \end{cases} \quad (9)$$

and we define  $\mathcal{CN}(\mathbf{x}_n^\tau; 0, \beta) = (\pi\beta)^{-M} \exp(-\beta^{-1} \|\mathbf{x}_n^\tau\|_2^2)$ .

<sup>1</sup>Note that we only consider one previous frame and one next frame for SI since the temporal correlation of device activity is modeled as a first-order Markov chain. An arbitrary number of adjacent frames can be considered if the device activity evolves according to an arbitrary stochastic process.

Under the above probabilistic model, the MMSE-optimal denoising function is given as

$$\boldsymbol{\eta}_{n,i}(\mathbf{r}_{n,i}^t, \mathcal{S}_n^t) = \mathbb{E}[\mathbf{x}_n^t | \mathbf{r}_{n,i}^t, \mathcal{S}_n^t]. \quad (10)$$

By substituting (10) into (6), the state  $\boldsymbol{\Sigma}_i^t$  in each iteration will also be a scaled identity matrix as  $\boldsymbol{\Sigma}_i^t = e_i^t \mathbf{I}$ ,  $\forall i, t$ , if the initial state is  $\boldsymbol{\Sigma}_0^t = e_0^t \mathbf{I}$ ,  $\forall i, t$ . The proof is similar to that in [2], [3]. With the above, the explicit expression of the MMSE-optimal denoising function can be given by the following Theorem.

**Theorem 1.** *The MMSE-optimal denoising function for user  $n$  in the vAMP framework with DSI can be represented as*

$$\boldsymbol{\eta}_{n,i}(\mathbf{r}_{n,i}^t, \mathcal{S}_n^t) = \frac{(1 + e_i^t/\beta)^{-1} \mathbf{r}_{n,i}^t}{1 + \phi_{n,i}^t(\mathbf{r}_{n,i}^t, \mathcal{S}_n^t)}, \quad (11)$$

where

$$\begin{aligned} \phi_{n,i}^t(\mathbf{r}_{n,i}^t, \mathcal{S}_n^t) &= v_{n,i}^t \times \frac{1-p_a}{p_a} \times \frac{p_{01} + (1-p_{01})v_{n,\infty}^{t-1}}{p_{11} + (1-p_{11})v_{n,\infty}^{t-1}} \\ &\times \frac{p_{01} + (1-p_{01})v_{n,\infty}^{t+1}}{p_{11} + (1-p_{11})v_{n,\infty}^{t+1}}, \end{aligned} \quad (12)$$

and  $v_{n,i}^t$  is the inverse LLR defined as

$$v_{n,i}^t = \frac{p(\mathbf{r}_{n,i}^t | \lambda_n^t = 0)}{p(\mathbf{r}_{n,i}^t | \lambda_n^t = 1)} = \left( \frac{\beta + e_i^t}{e_i^t} \right)^M \exp\left(-\Xi_i^t \|\mathbf{r}_{n,i}^t\|_2^2\right), \quad (13)$$

with  $\Xi_i^t = (e_i^t)^{-1} - (e_i^t + \beta)^{-1}$ . The inverse LLRs  $v_{n,\infty}^{t-1}$  and  $v_{n,\infty}^{t+1}$  are similarly calculated by following (13).

*Proof:* Please see Appendix A. ■

To gain insights from Theorem 1, we consider some special cases. First, when there is no temporal correlation in user activity, i.e.,  $p_{01} = p_{11} = p_a$ , the function (12) is simplified as  $\phi_{n,i}^t(\mathbf{r}_{n,i}^t, \mathcal{S}_n^t) = \frac{1-p_a}{p_a} v_{n,i}^t$ . Thus, the function in (11) reduces to the MMSE denoiser  $\boldsymbol{\eta}_{n,i}(\mathbf{r}_{n,i}^t) = \frac{(1+e_i^t/\beta)^{-1} \mathbf{r}_{n,i}^t}{1+v_{n,i}^t(1-p_a)/p_a}$  in [2], [3] without SI. Second, if we have  $v_{n,\infty}^\tau = 1$  for  $\tau = t-1$  or  $t+1$ , i.e., the device is equally likely to be active or inactive at frame  $\tau$ , then the SI from frame  $\tau$  provides no useful information for the estimation.

To get more insights, we consider the extreme case where the exact activities in the previous frame and the next frame are known, i.e., the corresponding SI is *perfect*. In this case, we have  $v_{n,\infty}^\tau = \infty$  if  $\lambda_n^\tau = 0$ , and  $v_{n,\infty}^\tau = 0$  otherwise, for  $\tau \in \{t-1, t+1\}$ . With perfect SI, then when user activity is fully correlated in time with  $p_{11} = 1$ , we have  $\lambda_n^t = \lambda_n \in \{0, 1\}$ ,  $\forall t$ . The MMSE-optimal denoising function becomes  $\boldsymbol{\eta}_{n,i}(\mathbf{r}_{n,i}^t, \mathcal{S}_n^t) = (1 + e_i^t/\beta)^{-1} \mathbf{r}_{n,i}^t$  if  $\lambda_n = 1$ , or  $\boldsymbol{\eta}_{n,i}(\mathbf{r}_{n,i}^t, \mathcal{S}_n^t) = \mathbf{0}$  if  $\lambda_n = 0$ . As such, the joint activity detection and channel estimation reduces to channel estimation only, and the channel estimator is a linear function that operates on each element of  $\mathbf{r}_{n,i}^t$  individually. This suggests that the performance of the algorithm is independent of the number of antennas.

When detecting the active users in the  $t$ th frame, the estimation results in the  $(t-1)$ th frame is already available and thus the SI  $\{v_{n,\infty}^{t-1}\}_{n=1}^N$  can be readily obtained. On the other hand, the SI from the  $(t+1)$ th frame need to be estimated.

In this work, we propose to employ the vAMP algorithm [2], [3] to perform coarse detection and estimation in the  $(t+1)$ th frame, then the estimation results of  $\{\mathbf{r}_{n,\infty}^{t+1}\}_{n=1}^N$  and  $e_{\infty}^{t+1}$  are used to obtain  $\{v_{n,\infty}^{t+1}\}_{n=1}^N$ . Finally, we perform joint activity detection and channel estimation in the  $t$ th frame based on the vAMP-SI algorithm with  $\{v_{n,\infty}^{t-1}\}_{n=1}^N$  and  $\{v_{n,\infty}^{t+1}\}_{n=1}^N$ .

### C. Activity Detector Design

The activity detection is performed based on the LLR test after the proposed algorithm converges. We denote  $H_0$  as the hypothesis that the device  $n$  is inactive with  $\lambda_n^t = 0$ , and denote  $H_1$  as the hypothesis otherwise. The Bayes-Risk activity decision rule is represented as

$$\xi_n^t = \log \left( \frac{p(\mathbf{r}_{n,\infty}^t, \mathcal{S}_n^t | \lambda_n^t = 1)}{p(\mathbf{r}_{n,\infty}^t, \mathcal{S}_n^t | \lambda_n^t = 0)} \right) \underset{H_0}{\overset{H_1}{\geq}} \iota^\xi, \quad (14)$$

where  $\xi_n^t$  is the LLR for device  $n$  and  $\iota^\xi$  is a predetermined decision threshold for all devices. Since the LLR  $\xi_n^t$  is a monotonic function on  $\|\mathbf{r}_{n,\infty}^t\|_2^2$ , the decision rule can be simplified as  $\|\mathbf{r}_{n,\infty}^t\|_2^2 \underset{H_0}{\overset{H_1}{\geq}} \iota_n^r$ .

**Theorem 2.** *The decision threshold of user  $n$  in the  $t$ th frame can be expressed as*

$$\iota_n^r = \frac{\iota^\xi + M \log \left( \frac{e_{\infty}^t + \beta}{e_{\infty}^t} \right) + \log \left( \frac{p_a}{1-p_a} \cdot \frac{\phi_{n,\infty}^t(\mathbf{r}_{n,\infty}^t, \mathcal{S}_n^t)}{v_{n,\infty}^t} \right)}{\Xi_{\infty}^t}. \quad (15)$$

where  $\phi_{n,\infty}^t(\mathbf{r}_{n,\infty}^t, \mathcal{S}_n^t)$  is given by (12).

*Proof:* The proof is similar to that of Theorem 1 and hence ignored. ■

Theorem 2 indicates that the SI from the previous and next frames has a great impact on the decision threshold setting. Similar to the insights derived from Theorem 1, if  $p_{01} = p_{11} = p_a$ , the activity detector will be reduced to that in [2], [3], where the SI is not utilized. When we have  $v_{n,\infty}^\tau = 1$  for  $\tau = t-1$  or  $t+1$ , no useful information is provided from the  $\tau$ th frame for activity detection.

### D. Discussion

Compared with the SI-aided MMV-AMP algorithm [9] that only exploits the single-sided information (SSI), our proposed algorithm can utilize the DSI. In particular, the SI from frame  $(t+1)$  is obtained by performing an extra vAMP estimation on  $\mathbf{X}^{t+1}$ . This, however, doubles the computation cost and adds one-frame detection delay. As shall be demonstrated in the next section, such extra complexity and delay can bring significant performance enhancement when the BS only has a few antennas.

### E. Extension to the Generalized Case

Here, we extend the proposed algorithm to the generalized case where the activity evolution of the device follows an arbitrary stochastic process. Since the activity in this case may not be only correlated with those in the previous frame and the next frame, we can consider a larger sliding window starting from the  $(t-T_l)$ th frame to the  $(t+T_r)$ th frame

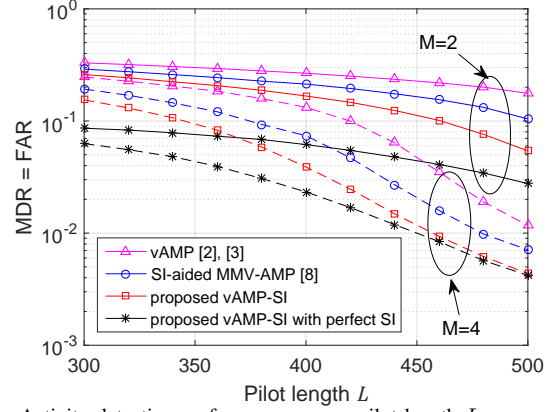


Fig. 2. Activity detection performance versus pilot length  $L$ .

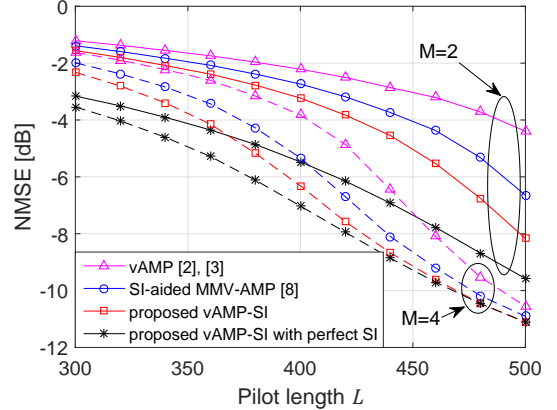


Fig. 3. Channel estimation performance versus pilot length  $L$ .

with  $\mathcal{T}_w^t = \{\tau | \tau = t - T_l, \dots, t + T_r, \tau \neq t\}$ . With the prior information of the activity evolution and the SI from the estimation results of all frames in  $\mathcal{T}_w^t$ , the MMSE-optimal denoising function and the decision threshold for each user  $n$  can be given by the following corollary.

**Corollary 1.** *In the generalized case where the activity evolution of the device follows an arbitrary stochastic process, the MMSE-optimal denoising function and the decision threshold for each user  $n$  in the  $t$ th frame are also written in the form of (11) and (15). While the function  $\phi_{n,i}^t(\mathbf{r}_{n,i}^t, \mathbf{s}_n^t)$  is modified as*

$$\phi_{n,i}^t(\mathbf{r}_{n,i}^t, \mathbf{s}_n^t) = \frac{\sum_{s \in \mathcal{S}_w} u_s \varphi_i^t(\mathbf{r}_{n,i}^t, \mathbf{P}_s) \prod_{\tau \in \mathcal{T}_w^t} \varphi_{\infty}^{\tau}(\mathbf{r}_{n,\infty}^{\tau}, \mathbf{P}_s)}{\sum_{s \in \mathcal{S}_w} u_s \varphi_i^t(\mathbf{r}_{n,i}^t, \mathbf{P}_s) \prod_{\tau \in \mathcal{T}_w^t} \varphi_{\infty}^{\tau}(\mathbf{r}_{n,\infty}^{\tau}, \mathbf{P}_s)}. \quad (16)$$

where  $\varphi_i^t(\mathbf{r}_{n,i}^t, \mathbf{P}_s)$  and  $\varphi_{\infty}^{\tau}(\mathbf{r}_{n,\infty}^{\tau}, \mathbf{P}_s)$  are defined in (20).

*Proof:* The proof of this corollary is similar to the proof of Theorem 1 and hence ignored. ■

Based on the corollary, we can see that the MMSE-optimal denoising function can be designed in the explicit expression once the occurrence probability  $u_s$  is available even if the activity evolution cannot be explicitly characterized.

## V. SIMULATION RESULTS

We consider the system containing  $N = 2000$  devices. The signal-to-noise ratio is defined as  $\text{SNR} = \frac{\beta}{\sigma_w^2}$  and is set to  $\text{SNR} = -10\text{dB}$ . We set  $p_{01} = 1/16$  and  $p_{11} = 3/4$  if not

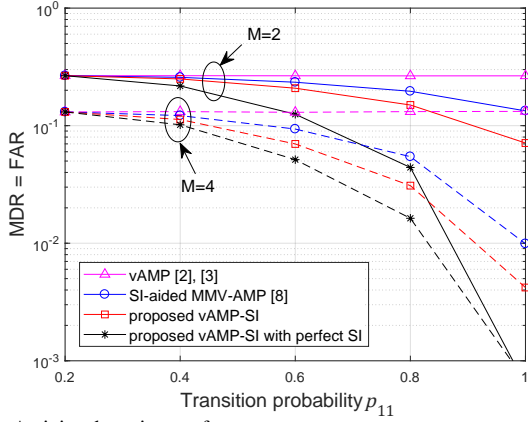


Fig. 4. Activity detection performance versus  $p_{11}$ .

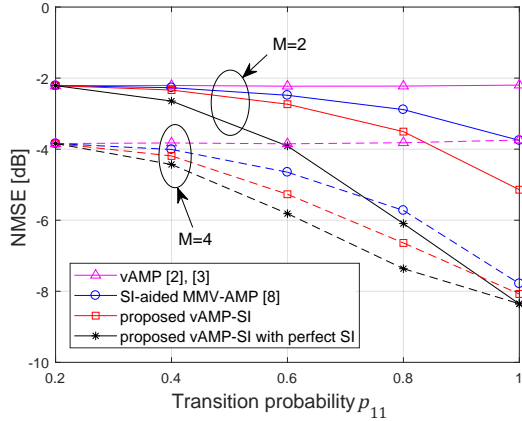


Fig. 5. Channel estimation performance versus  $p_{11}$ .

specified otherwise, then we have  $p_a = 1/5$ . The joint activity detection and channel estimation is performed in  $T = 8$  consecutive frames. The missed detection ratio (MDR) and the false alarm ratio (FAR) are used as the performance metrics for activity detection, the normalized mean-squared error (NMSE) is used as the performance metric for channel estimation. The vAMP algorithm [2], [3] and the SI-aided MMV-AMP algorithm [9] are considered as benchmarks. We also evaluate the proposed algorithm with perfect SI as performance bound.

Fig. 2 and Fig. 3 show the activity detection and the channel estimation performance, respectively, at different pilot lengths. Here, we have set  $\text{MDR} = \text{FAR}$  by carefully selecting the decision threshold  $\nu_n^r$ . We observe that the proposed algorithm can significantly outperform the state-of-the-art algorithms. We also observe that the performance gap to the lower bound with perfect SI reduces when the antenna number  $M$  and the pilot length  $L$  increases. In particular, when  $M = 4$  and  $L = 500$ , the proposed vAMP-SI algorithm nearly converges to the ideal case. This indicates that the proposed algorithm can better exploit the temporal correlation in device activity to improve the performance.

Fig. 4 and Fig. 5 illustrate the performance of the proposed algorithm under different transition probabilities  $p_{11}$ , where the active probability is fixed to be  $p_a = 1/5$ . As mentioned, when  $p_{01} = p_{11} = p_a$ , the device activities in different frames are temporally independent. Thus, we consider that  $p_{11}$  ranges from 0.2 to 1 in the simulations. It is observed that by exploiting the double-sided information, the proposed vAMP-SI algorithm outperforms considerably the existing SI-

aided MMV-AMP. Similar to the result in Fig. 2 and Fig. 3, the performance of the proposed algorithm is closer the ideal performance with perfect SI by increasing  $M$ . When  $p_{11} = 1$ , the proposed algorithm with perfect SI has the same channel estimation performance for  $M = 2$  and  $M = 4$ . This observation validates the discussion in Section IV-B that the channel estimation performance in this limiting case is irrelevant to the number of antennas.

## VI. CONCLUSION

This paper proposes to extract the SI from the estimation results in both the previous frame and the next frame for joint activity detection and channel estimation in temporal-correlated massive access. We introduce a sliding-window detection strategy and develop the vAMP-SI algorithm to exploit the double-sided information. The numerical results have validated that the proposed algorithm can achieve superior performance over the start-of-the-art algorithms. This work considers a block fading channel model, while the channel may also evolves according to a stochastic process and can be exploited in the algorithm design.

## APPENDIX A PROOF OF THEOREM 1

The MMSE-optimal denoising function can be written as

$$\begin{aligned} \eta_{n,i}(\mathbf{r}_{n,i}^t, \mathcal{S}_n^t) &\triangleq \mathbb{E}[\mathbf{x}_{n,i}^t | \mathbf{r}_{n,i}^t, \mathcal{S}_n^t] \\ &= \sum_{s \in \mathcal{P}_w} \mathbf{E}[\mathbf{x}_{n,i}^t | \mathbf{r}_{n,i}^t, \mathcal{S}_n^t, \mathbf{P}_s] p(\mathbf{P}_s | \mathbf{r}_{n,i}^t, \mathcal{S}_n^t), \end{aligned} \quad (17)$$

where  $\mathcal{P}_w = \{s | \lambda_n^t = 1 \text{ in } \mathbf{P}_s\}$  is the set containing the indexes of all activity patterns where  $\lambda_n^t = 1$ . For  $s \in \mathcal{P}_w$ , we can obtain

$$\begin{aligned} \mathbf{E}[\mathbf{x}_{n,i}^t | \mathbf{r}_{n,i}^t, \mathcal{S}_n^t, \mathbf{P}_s] &\stackrel{(a)}{=} \mathbb{E}[\mathbf{x}_{n,i}^t | \mathbf{r}_{n,i}^t = \mathbf{h}_n^t + \sqrt{e_i^t} \mathbf{d}_n^t] \\ &= (1 + e_i^t / \beta)^{-1} \mathbf{r}_{n,i}^t, \end{aligned} \quad (18)$$

where  $\stackrel{(a)}{=}$  is the fact that all vectors in  $\{\mathbf{h}_n^\tau\}_{\tau=t-1}^{t+1}$  and  $\{\mathbf{d}_n^\tau\}_{\tau=t-1}^{t+1}$  are mutually independent. Then the probability  $p(\mathbf{P}_s | \mathbf{r}_{n,i}^t, \mathcal{S}_n^t)$  can be calculated as

$$\begin{aligned} p(\mathbf{P}_s | \mathbf{r}_{n,i}^t, \mathcal{S}_n^t) &= \frac{p(\mathbf{r}_{n,i}^t, \mathcal{S}_n^t | \mathbf{P}_s) p(\mathbf{P}_s)}{p(\mathbf{r}_{n,i}^t, \mathcal{S}_n^t)} \\ &= \frac{u_s \varphi_i^t(\mathbf{r}_{n,i}^t, \mathbf{P}_s) \prod_{\tau \in \mathcal{T}_w \setminus t} \varphi_\infty^\tau(\mathbf{r}_{n,\infty}^\tau, \mathbf{P}_s)}{p(\mathbf{r}_{n,i}^t, \mathcal{S}_n^t)}, \end{aligned} \quad (19)$$

where

$$\varphi_i^t(\mathbf{r}_{n,i}^t, \mathbf{P}_s) = \begin{cases} \mathcal{CN}(\mathbf{r}_{n,i}^t; 0, e_i^t), & \text{if } \lambda_n^t = 0 \text{ in } \mathbf{P}_s, \\ \mathcal{CN}(\mathbf{r}_{n,i}^t; 0, e_i^t + \beta), & \text{otherwise,} \end{cases} \quad (20)$$

$$\begin{aligned} p(\mathbf{r}_{n,i}^t, \mathcal{S}_n^t, \mathbf{P}_s) &= \sum_{s=1}^8 p(\mathbf{r}_{n,i}^t, \mathcal{S}_n^t | \mathbf{P}_s) p(\mathbf{P}_s) \\ &= \sum_{s=1}^8 \left[ u_s \varphi_i^t(\mathbf{r}_{n,i}^t, \mathbf{P}_s) \left( \prod_{\tau \in \mathcal{T}_w \setminus t} \varphi_\infty^\tau(\mathbf{r}_{n,\infty}^\tau, \mathbf{P}_s) \right) \right]. \end{aligned} \quad (21)$$

By inserting the above functions (18), (19) and (21) into (17), the MMSE-optimal denoising function in the vAMP-SI algorithm can be finally simplified in the form of (11).

## REFERENCES

- [1] L. Liu, E. G. Larsson, W. Yu, P. Popovski, C. Stefanovic, and E. de Carvalho, "Sparse signal processing for grant-free massive connectivity: A future paradigm for random access protocols in the internet of things," *IEEE Signal Process. Mag.*, vol. 35, no. 5, pp. 88–99, Sep. 2018.
- [2] Z. Chen, F. Sotiriou, and W. Yu, "Sparse activity detection for massive connectivity," *IEEE Trans. Signal Process.*, vol. 66, no. 7, pp. 1890–1904, April 2018.
- [3] L. Liu and W. Yu, "Massive connectivity with massive MIMO-Part I: Device activity detection and channel estimation," *IEEE Trans. Signal Process.*, vol. 66, no. 11, pp. 2933–2946, June 2018.
- [4] K. Senel and E. G. Larsson, "Grant-free massive MTC-enabled massive MIMO: A compressive sensing approach," *IEEE Trans. Commun.*, vol. 66, no. 12, pp. 6164–6175, Dec 2018.
- [5] M. Ke, Z. Gao, Y. Wu, X. Gao, and R. Schober, "Compressive sensing-based adaptive active user detection and channel estimation: Massive access meets massive mimo," *IEEE Trans. Signal Process.*, vol. 68, pp. 764–779, 2020.
- [6] A. Fengler, S. Haghshatshoar, P. Jung, and G. Caire, "Non-bayesian activity detection, large-scale fading coefficient estimation, and unsourced random access with a massive mimo receiver," *IEEE Trans. Inf. Theory*, vol. 67, no. 5, pp. 2925–2951, 2021.
- [7] J. C. Jiang and H. M. Wang, "Massive random access with sporadic short packets: Joint active user detection and channel estimation via sequential message passing," *IEEE Trans. Wireless Commun.*, pp. 1–1, 2021.
- [8] W. Zhu, M. Tao, and Y. Guan, "Joint user activity detection and channel estimation for temporal-correlated massive access," in *Proc. IEEE Int. Conf. Commun.*, 2021, pp. 1–6.
- [9] Q. Wang, L. Liu, S. Zhang, and F. C. M. Lau, "On massive iot connectivity with temporally-correlated user activity," in *Proc. IEEE Int. Symp. Inf. Theory*, 2021, pp. 3020–3025.
- [10] A. Ma, Y. Zhou, C. Rush, D. Baron, and D. Needell, "An approximate message passing framework for side information," *IEEE Trans. Signal Process.*, vol. 67, no. 7, pp. 1875–1888, 2019.